Vol 463|14 January 2010|doi:10.1038/nature08707

LETTERS

Dominant control of the South Asian monsoon by orographic insulation versus plateau heating

William R. Boos[1] & Zhiming Kuang[1,2]

The Tibetan plateau, like any landmass, emits energy into the atmosphere in the form of dry heat and water vapour, but its mean surface elevation is more than 5 km above sea level. This elevation is widely held to cause the plateau to serve as a heat source that drives the South Asian summer monsoon, potentially coupling uplift of the plateau to climate changes on geologic timescales[1–5]. Observations of the present climate, however, do not clearly establish the Tibetan plateau as the dominant thermal forcing in the region: peak upper-tropospheric temperatures during boreal summer are located over continental India, south of the plateau. Here we show that, although Tibetan plateau heating locally enhances rainfall along its southern edge in an atmospheric model, the large-scale South Asian summer monsoon circulation is otherwise unaffected by removal of the plateau, provided that the narrow orography of the Himalayas and adjacent mountain ranges is preserved. Additional observational and model results suggest that these mountains produce a strong monsoon by insulating warm, moist air over continental India from the cold and dry extratropics. These results call for both a reinterpretation of how South Asian climate may have responded to orographic uplift, and a re-evaluation of how this climate may respond to modified land surface and radiative forcings in coming decades.

The Tibetan plateau has long been held to serve as an elevated heat source that drives the thermally direct circulation of the South Asian summer monsoon, with air at a given level of the atmosphere thought to be heated to higher temperatures over the plateau than over adjacent non-elevated surfaces[1,2,6]. Often cited in support of this idea is the fact that the intensity and northward extent of monsoon rains were greatly reduced in general circulation models (GCMs) in which all elevated topography was eliminated[3,7–11]. Together with proxies for past winds and rainfall, these results have been used to argue that tectonic uplift of the plateau, which may have occurred millions of years after Himalayan uplift, caused a large increase in Asian monsoon intensity[4,12,13]. The idea that the thermal forcing of the Tibetan plateau drives the South Asian monsoon is sufficiently widespread to cause worry that changes in its surface temperature, glacial cover and vegetation in a warming climate might alter monsoon intensity in coming decades[5].

However, model tests that show a dramatic monsoon weakening in the absence of all topography do not distinguish the role of the Himalayas from that of the horizontally extensive Tibetan plateau. Furthermore, the thermodynamic structure of the troposphere does not clearly establish the Tibetan plateau as the dominant heat source for the South Asian summer monsoon: upper-tropospheric temperatures peak south of the plateau during boreal summer (Fig. 1a). The upper-tropospheric high pressure system often called the Tibetan High is also centred south of the plateau (Supplementary Information). Some authors have attempted to reconcile these facts with the supposed dominant role of plateau heating by assuming that the plateau acts as a sensible heat pump, driving local ascent that causes low-level moist air south of the plateau to converge and condense, producing latent heating that in turn drives the large-scale monsoon flow[14]. However, such a mechanism would not explain why peak upper-tropospheric temperatures are centred over northern India, about 1,000 km west of the peak precipitation. Furthermore, we present model results below to show that the large-scale monsoon flow is insensitive to the removal of plateau heating.

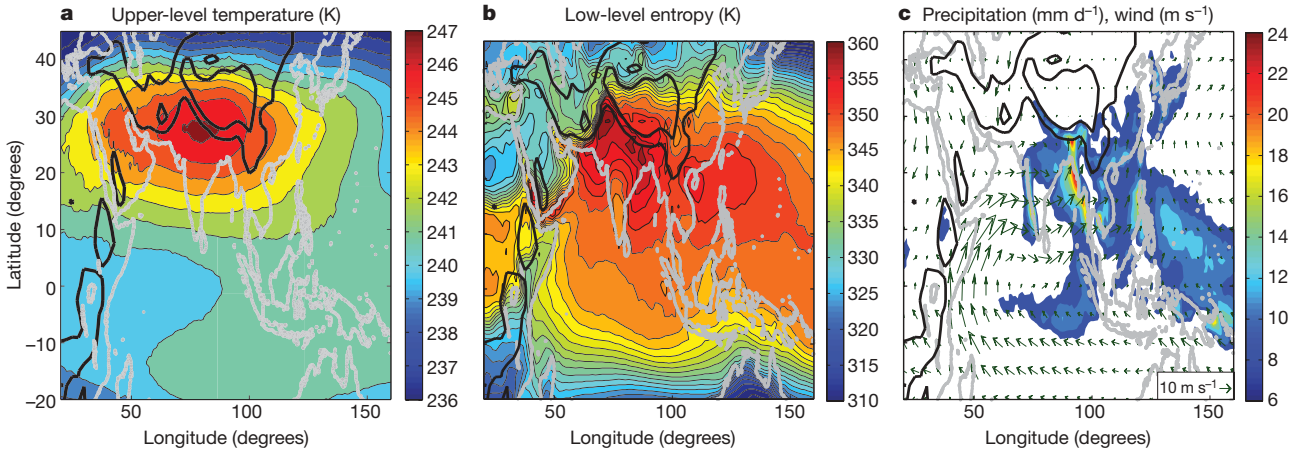

Figure 1 | Observational estimates of June–August thermodynamic structure, precipitation and wind. **a**, Satellite-based (AIRS) estimate of mass-weighted vertical mean temperature for 175–450 hPa. **b**, ERA40 equivalent potential temperature on a terrain-following model level about 20 hPa above the surface. **c**, TRMM precipitation rate (colour shading) and ERA40 850 hPa winds (vectors). In all panels, grey lines denote coasts and thick black contours surround surface pressures lower than 900 hPa and 700 hPa. The contour interval is 1 K in **a**, 2 K in **b** and 2 mm d^{-1} in **c**.

[1]Department of Earth and Planetary Sciences, [2]School of Engineering and Applied Sciences, Harvard University, Cambridge, Massachusetts 02138, USA.

©2010 Macmillan Publishers Limited. All rights reserved

An alternative hypothesis for the role of topography in South Asian climate is suggested by the fact that peak upper-level temperatures lie directly over the highest near-surface moist entropy, measured in terms of the equivalent potential temperature, θ_e, on a terrain-following surface of the ECMWF Reanalysis 40 (ERA40) data set (Fig. 1b). Although the ERA40 values are a blend of data and model results, the location of the subcloud θ_e maximum is consistent with measurements from twice-daily balloon soundings (Fig. 2a). Subcloud entropy is expected to be coupled with upper-tropospheric temperatures when the fast processes of cumulus convection, with timescales of the order of an hour, are in statistical equilibrium with the slower thermal forcings of radiation, surface heat fluxes and large-scale flow[15,16]. The fact that the maximum subcloud θ_e is located south of the Himalayas suggests that the thermal forcing of continental India may be more important than that of the Tibetan plateau in setting the location and amplitude of peak free-tropospheric temperatures. Furthermore, the coincidence of sharp gradients of subcloud θ_e with mountain ranges suggests that topography may create a strong South Asian monsoon by insulating high-entropy air over India from low-entropy extratropical air. Although the idea that the intensity and poleward extent of monsoons may be limited by the advection of cold and dry air from the extratropics exists in the literature[17,18], the ability of topography to influence the large-scale, interhemispheric South Asian monsoon through this mechanism has not been explored (Supplementary Information).

Thermodynamic profiles obtained from twice-daily balloon soundings of the atmosphere suggest that the direct heating of the Tibetan plateau may be largely confined to a local dry boundary layer. Over the plateau and over regions of India with the highest upper-tropospheric temperatures, the vertical temperature structure roughly follows that of a moist adiabat (Fig. 2). In early morning, temperatures are warmer over northern India than over the plateau up to a pressure level of about 250 hPa. A high-amplitude diurnal cycle in temperature extends to about 450 hPa over the plateau and reverses the mid-tropospheric horizontal temperature gradient during late afternoon. Temperatures remain higher over India, however, in the upper troposphere between 450 hPa and 250 hPa. Above the 250 hPa pressure level, temperatures are cooler over India; this is presumably associated with adiabatic cooling due to lifting above a thick warm layer, and is consistent with widely observed negative correlations between vertically averaged free-tropospheric temperatures and temperatures near the tropopause[19]. Sounding data also show that, in the diurnal and summer mean, energy available for precipitating convection is large over India while it is near zero over Tibet. This energy is non-zero but small for some of the southern plateau soundings during late afternoon (not shown). These findings are all consistent with the thermal effects of the plateau being largely confined to a dry diurnal boundary layer, with maximum upper-tropospheric temperatures located over northern India where precipitating convection thermodynamically couples the upper troposphere to the air of the highest-entropy subcloud layer.

If topography produces a strong South Asian summer monsoon primarily by protecting warm and moist tropical air from the cold and dry extratropics, then a band of narrow mountain ranges should be sufficient to produce a strong monsoon. We have tested this hypothesis using an atmospheric GCM with modified topography and land surface albedo (see Methods for model details). The modified distributions of topography and albedo are not intended to represent actual configurations from the geologic past, but to facilitate investigation of the processes by which topography alters the monsoon. The model is integrated with prescribed, modern-day sea surface temperature (SST) in order to isolate the effects of topography on atmospheric dynamics; it is understood that this approach will not capture indirect effects of topographic changes manifested through modified ocean circulation.

A control model integration with modern-day topography produces distributions of upper-tropospheric temperature and subcloud entropy with maxima having positions similar to those observed (Fig. 3a). Peak temperatures and entropies are slightly lower than observed, but the match seems sufficient to qualify the model as an adequate control. Model precipitation exhibits some bias, with overly strong maxima near the western Ghats and the southern Himalayas, and an overly weak maximum near the west coast of the Indochina peninsula. But these biases are no larger than those seen in many GCMs deemed to adequately simulate the Asian summer monsoon[20], and the simulated precipitation and thermal maxima are located near the correct latitudes.

In an integration with all surface elevations set to zero but with other surface properties unchanged, peak upper-tropospheric temperatures are reduced and shifted about 1,500 km southeast of their position in the control run (Fig. 3b). Peak subcloud entropies are also displaced a similar distance south of their position in the control run, in a zonally elongated band coincident with peak upper-tropospheric temperatures. The gradient between tropical and extratropical subcloud entropies is weaker than in the control run, and is no longer coincident with any

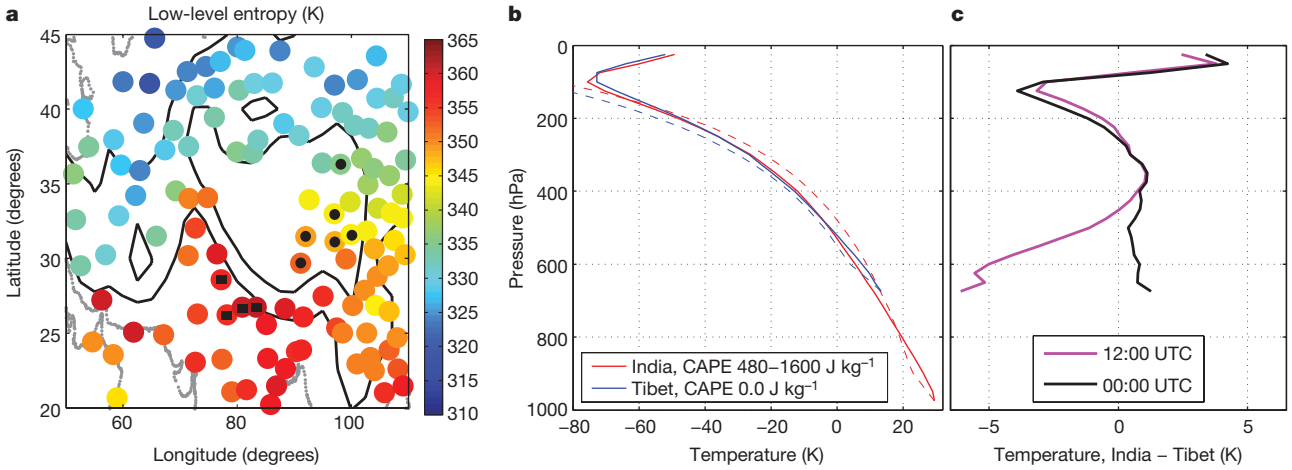

Figure 2 | Thermodynamic structure from balloon soundings for June–August. a, Equivalent potential temperature within 25 hPa of the surface at radiosonde sites over and around the Tibetan plateau. Black squares and circles mark the stations used to produce the vertical profiles for India and Tibet, respectively, shown in **b** and **c**. **b**, Daily mean profiles of temperature, averaged over Indian stations with the warmest upper-tropospheric temperature (solid red line) and Tibetan plateau stations with sufficient upper-level data (solid blue line). Dashed lines are dry adiabats from the lowest sounding level up to the lifted condensation level, and moist pseudoadiabats thereafter. Convective available potential energy (CAPE) for each sounding is displayed, with the two values for India corresponding to calculations performed using reversible and pseudoadiabatic ascent. **c**, Mean temperature difference between the Indian and Tibetan plateau sites, with positive values denoting air that is warmer over Indian sites. The black line denotes values at 00:00 UTC (5:30 AM India local time) and the magenta line at 12:00 UTC (5:30 PM India local time).

©2010 Macmillan Publishers Limited. All rights reserved

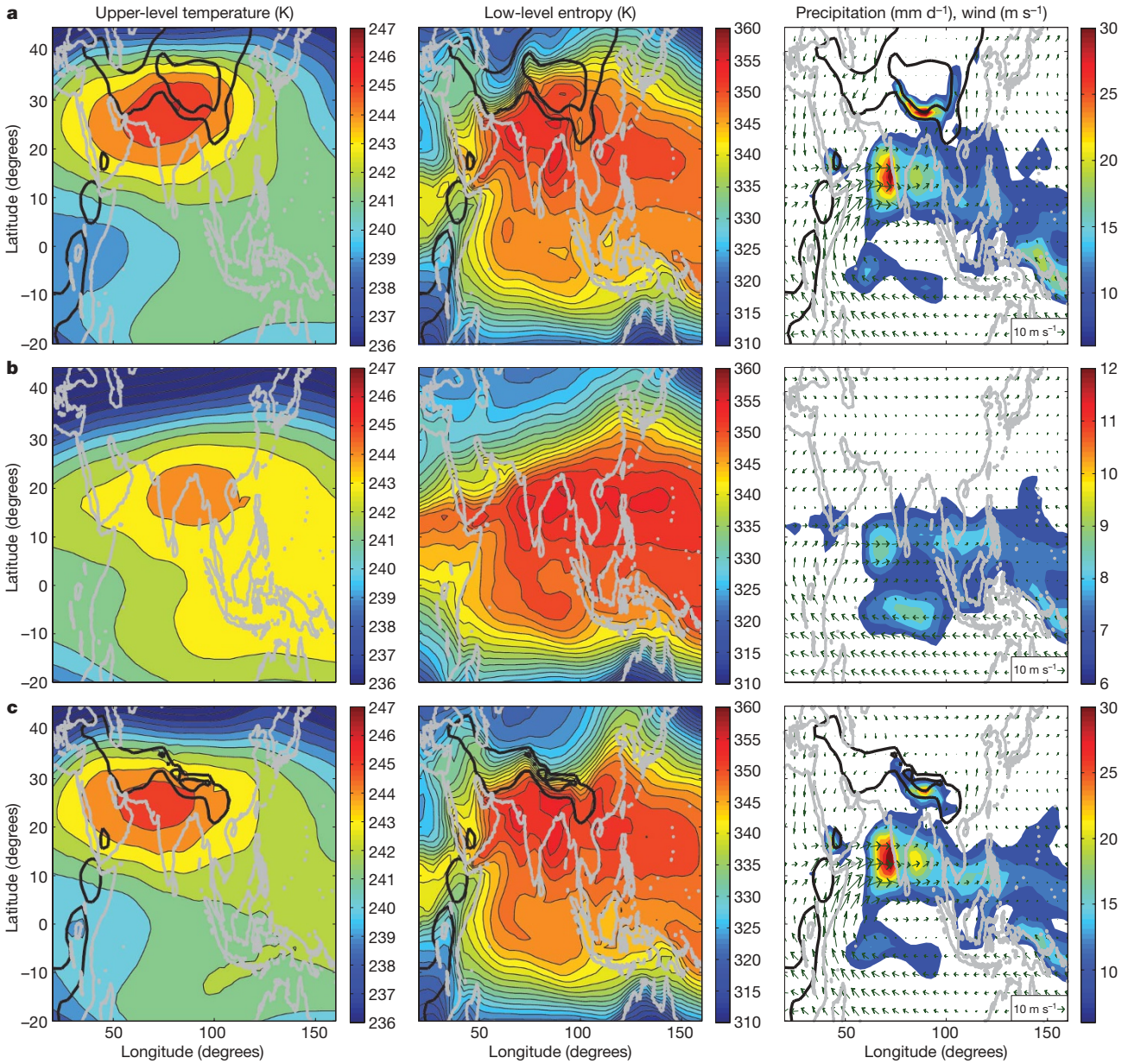

Figure 3 | Thermodynamic structure, precipitation and wind from the atmospheric model. All panels are for June–August and as in Fig. 1 but for the model run with **a**, standard topography, **b**, no elevated topography, and **c**, surface elevations north of the Himalayas set to zero.

geographic feature. In current observations, peak upper-tropospheric temperatures are centred at a similar location over the Indochina peninsula before the onset of the Indian summer monsoon[21], suggesting that this monsoon is largely absent in the model without elevated topography. Precipitation maxima and low-level westerly winds are strongly reduced and shifted towards the Equator compared to the control run, with the Himalayan precipitation maximum entirely eliminated. These precipitation changes are similar to those seen in other model studies where elevated topography was eliminated[8,11].

The two integrations just discussed show that topography produces a strong South Asian summer monsoon, but they do not distinguish between the effects of the Tibetan plateau and other topographic features. Thus, we also performed an integration in which the bulk of the plateau was removed but all other orography was unchanged, including mountain ranges west and south of the plateau (Fig. 3c shows topographic contours). In this run, subcloud entropies south of the Himalayas had a distribution similar to that in the control run, even though entropies were considerably lower in the region formerly occupied by the Tibetan plateau. This suggests that although subcloud entropies do increase with surface elevation, consistent with previous studies[22], this effect is not strong enough to make the plateau the site of a global entropy maximum. Peak upper-tropospheric temperatures in this run are displaced slightly southwest of their position in the control run, but they still lie over northern India and have an amplitude near that in the control run. The precipitation distribution is similar to that in the control run, except for a reduction in rainfall over the southern Himalayas and East Asia. The horizontally extensive Tibetan plateau thus enhances upper-level temperatures and rainfall locally along the southern and eastern edges of the plateau in this model, but otherwise has a minor effect on precipitation, low-level wind, and the thermodynamic structure of the large-scale South Asian monsoon. It similarly has a minor effect on maxima in the free-tropospheric vertical velocity field (Supplementary Information).

These results are consistent with the hypothesis that mountains south and west of the plateau produce a strong monsoon by insulating the thermal maximum over India from the extratropics, but we have not yet tested the effect of plateau heating while controlling for the mechanical effects of orography. To assess the importance of

©2010 Macmillan Publishers Limited. All rights reserved

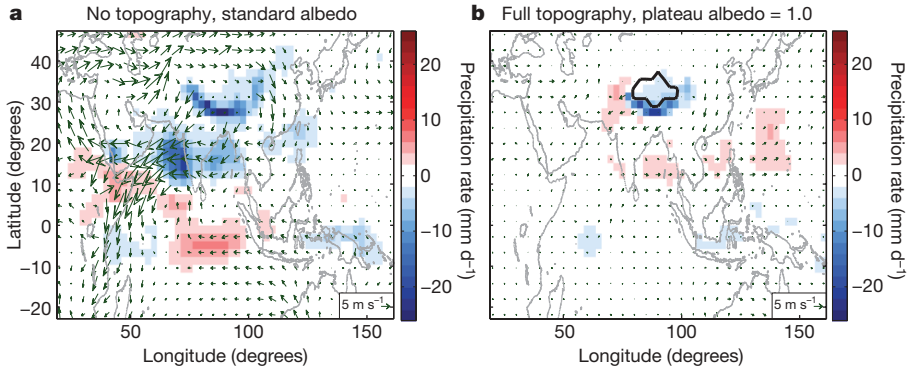

Figure 4 | Results from model runs with modified topography and surface albedo. Shading shows precipitation and arrows show 850 hPa horizontal wind, both as anomalies relative to the control run with standard topography and albedo. **a**, Run with no elevated topography but standard surface albedo (that is, the same run shown in Fig. 3b). **b**, Run with standard topography but with the Tibetan plateau assigned a surface shortwave albedo of unity. The thick black contour surrounds regions where the surface albedo was modified.

regional surface heat fluxes without altering the ability of topography to block flow or induce low-level moisture convergence, we integrated the same atmospheric model with standard topography but with modified land surface albedo. In a run with the surface albedo of the Tibetan plateau set to unity, all solar radiation incident on the plateau is reflected, producing near zero sensible and latent heat flux on the plateau surface. This produced a strong reduction in precipitation south of the plateau along the Himalayas, but almost no change in the low-level wind (Fig. 4b). A slight increase in precipitation occurred southwest of the plateau and over the ocean near 15° N, suggesting that plateau heating may actually shift rainfall from some parts of South Asia into the Himalayas. But compared to the effects of removing all topography (Fig. 4a), surface heat fluxes from the plateau exert a primarily local effect on rainfall near the Himalayas, with negligible influence on the circulation.

Additional model integrations were performed to confirm that the South Asian monsoon was most sensitive to the band of mountains west and south of the plateau, and not some other topographic feature (Supplementary Information). The comparatively low mountains on the west coasts of India and the Indochina peninsula did enhance model precipitation on their upwind side and strengthen the monsoon circulation, consistent with a previous study[23], but this effect was not as large as that caused by the mountains south and west of the plateau.

In contrast to its effects on South Asian summer climate, the Tibetan plateau may be very important for East Asian climate. It is likely that the mechanical effects of plateau orography set the position of the jet stream and the dynamics of low-level flow that advect moisture into East Asia[24–27]. Such effects may be tied to jet stream and frontal dynamics that are extratropical in nature, rather than the tropical Hadley circulation dynamics thought relevant for the South Asian summer monsoon, and are not explored here. Finally, we emphasize that surface elevations used in our model were chosen to facilitate investigation of atmospheric mechanisms and not to represent likely configurations of past orography. Our choice of prescribed modern SST was similarly made to simplify investigation of the mechanism by which orography alters atmospheric dynamics. Additional work is needed to assess how the evolution of climate may be coupled with plateau uplift, the formation of zonally elongated mountain ranges, and changes in ocean circulation on geologic timescales.

METHODS SUMMARY

Boreal summer (June–August) climatologies of upper-tropospheric temperature were obtained from the Atmospheric Infrared Sounder (AIRS level 3, version 5) for 2003–08. Low-level winds and subcloud entropies were obtained from the European Centre for Medium-Range Weather Forecasts (ECMWF) Reanalysis 40 (ERA40, ref. 28) for 1979–2002, and precipitation from the Tropical Rainfall Measuring Mission (TRMM) 3B43V6 data set for 1998–2006, both provided by the National Center for Atmospheric Research (NCAR). Radiosonde data were taken from the Integrated Global Radiosonde Archive[29], and only stations having data at both 00:00 and 12:00 UTC for June–August 1970–2008 were used. All mentions of entropy in this paper refer to moist entropy, represented in terms of equivalent potential temperature[30].

Model integrations used the Community Atmospheric Model (CAM) version 3.5.18 (ref. 31). This interim version was chosen because the most recent public release (CAM 3.1) exhibited considerable bias in its simulation of the South Asian summer monsoon. Runs were started from initial conditions on 1 September 1992, with climatologies calculated for the following five June–August periods. Observed SST and sea ice for the same period were prescribed. Topography was modified by changing only the prescribed surface elevations, leaving unchanged all other fixed properties of the surface, including soil colour and vegetation. An additional integration was performed using standard topography but with the surface shortwave albedo set to unity on the Tibetan plateau.

Full Methods and any associated references are available in the online version of the paper at www.nature.com/nature.

Received 28 April; accepted 18 November 2009.

1. Flohn, H. Hochgebirge und allgemeine Zirkulation. II. Die Gebirge als Wärmequellen. *Arch. Meteorol. Geophys. Bioklimatol. A* **5**, 265–279 (1953).
2. Flohn, H. *Contributions to a Meteorology of the Tibetan Highlands* (Tech. Rep. 130, Colorado State Univ., 1968).
3. Hahn, D. G. & Manabe, S. The role of mountains in the South Asian monsoon circulation. *J. Atmos. Sci.* **32**, 1515–1541 (1975).
4. Molnar, P., England, P. & Martinod, J. Mantle dynamics, uplift of the Tibetan Plateau, and the Indian monsoon. *Rev. Geophys.* **31**, 357–396 (1993).
5. Qiu, J. China: The third pole. *Nature* **454**, 393–396 (2008).
6. Li, C. & Yanai, M. The onset and interannual variability of the Asian summer monsoon in relation to land-sea thermal contrast. *J. Clim.* **9**, 358–375 (1996).
7. Ruddiman, W. & Kutzbach, J. Forcing of late Cenozoic Northern Hemisphere climate by plateau uplift in southern Asia and the American West. *J. Geophys. Res.* **94**, 18409–18427 (1989).
8. Prell, W. & Kutzbach, J. Sensitivity of the Indian monsoon to forcing parameters and implications for its evolution. *Nature* **360**, 647–652 (1992).
9. Chakraborty, A., Nanjundiah, R. & Srinivasan, J. Role of Asian and African orography in Indian summer monsoon. *Geophys. Res. Lett.* **29**, 50–51 (2002).
10. Abe, M., Kitoh, A. & Yasunari, T. Evolution of the Asian summer monsoon associated with mountain uplift: simulation with the MRI atmosphere-ocean coupled GCM. *J. Meteorol. Soc. Jpn* **81**, 909–933 (2003).
11. Yasunari, T., Saito, K. & Takata, K. Relative roles of large-scale orography and land surface processes in the global hydroclimate. Part I: impacts on monsoon systems and the tropics. *J. Hydrometeorol.* **7**, 626–641 (2006).
12. Raymo, M. & Ruddiman, W. Tectonic forcing of late Cenozoic climate. *Nature* **359**, 117–122 (1992).
13. An, Z., Kutzbach, J., Prell, W. & Porter, S. Evolution of Asian monsoons and phased uplift of the Himalaya-Tibetan plateau since Late Miocene times. *Nature* **411**, 62–66 (2001).
14. Yanai, M. & Wu, G. in *The Asian Monsoon* (ed. Wang, B.) 513–549 (Springer, 2006).
15. Sarachik, E. Tropical sea surface temperature: an interactive one-dimensional atmosphere-ocean model. *Dyn. Atmos. Oceans* **2**, 455–469 (1978).
16. Emanuel, K. A., Neelin, J. D. & Bretherton, C. S. On large-scale circulations in convecting atmospheres. *Q. J. R. Meteorol. Soc.* **120**, 1111–1143 (1994).
17. Chou, C., Neelin, J. & Su, H. Ocean-atmosphere-land feedbacks in an idealized monsoon. *Q. J. R. Meteorol. Soc.* **127**, 1869–1892 (2001).

©2010 Macmillan Publishers Limited. All rights reserved

18. Chakraborty, A., Nanjundiah, R. & Srinivasan, J. Theoretical aspects of the onset of Indian summer monsoon from perturbed orography simulations in a GCM. *Ann. Geophys.* **24,** 2075–2089 (2006).
19. Holloway, C. & Neelin, J. The convective cold top and quasi equilibrium. *J. Atmos. Sci.* **64,** 1467–1487 (2007).
20. Lin, J. *et al.* Subseasonal variability associated with Asian summer monsoon simulated by 14 IPCC AR4 coupled GCMs. *J. Clim.* **21,** 4541–4567 (2008).
21. Boos, W. R. & Emanuel, K. A. Annual intensification of the Somali jet in a quasi-equilibrium framework: observational composites. *Q. J. R. Meteorol. Soc.* **135,** 319–335 (2009).
22. Molnar, P. & Emanuel, K. A. Temperature profiles in radiative-convective equilibrium above surfaces at different heights. *J. Geophys. Res.* **104,** 24265–24272 (1999).
23. Xie, S., Xu, H., Saji, N., Wang, Y. & Liu, W. Role of narrow mountains in large-scale organization of Asian monsoon convection. *J. Clim.* **19,** 3420–3429 (2006).
24. Liang, X.-Z. & Wang, W.-C. Associations between China monsoon rainfall and tropospheric jets. *Q. J. R. Meteorol. Soc.* **124,** 2597–2623 (1998).
25. Murakami, T. Orographic influence of the Tibetan Plateau on the Asiatic winter monsoon circulation. Part I: large-scale aspects. *J. Meteorol. Soc. Jpn* **59,** 66–84 (1981).
26. Zhou, Y., Gao, S. & Shen, S. S. P. A diagnostic study of formation and structures of the Meiyu front system over East Asia. *J. Meteorol. Soc. Jpn* **82,** 1565–1576 (2004).
27. Held, I., Ting, M. & Wang, H. Northern winter stationary waves: theory and modeling. *J. Clim.* **15,** 2125–2144 (2002).
28. Uppala, S. *et al.* The ERA-40 re-analysis. *Q. J. R. Meteorol. Soc.* **131,** 2961–3012 (2005).
29. Durre, I., Russell, S. V. & Wuertz, D. B. Overview of the Integrated Global Radiosonde Archive. *J. Clim.* **19,** 53–68 (2006).
30. Emanuel, K. *Atmospheric Convection* (Oxford Univ. Press, 1994).
31. Collins, W. *et al.* The formulation and atmospheric simulation of the Community Atmosphere Model: CAM3. *J. Clim.* **19,** 2144–2161 (2006).

Supplementary Information is linked to the online version of the paper at www.nature.com/nature.

Acknowledgements We thank P. Molnar for conversations motivating this work. Computing time was provided by the NCAR, which is sponsored by the NSF. W.R.B. was supported by the Reginald A. Daly Postdoctoral Fellowship in the Department of Earth and Planetary Sciences at Harvard University, and the John and Elaine French Environmental Fellowship at the Harvard University Center for the Environment. Z.K. was supported by NSF grant ATM-0754332.

Author Contributions Both authors contributed to designing the research and interpreting results. W.R.B. performed the observational analyses and model runs, and wrote the manuscript.

Author Information Reprints and permissions information is available at www.nature.com/reprints. The authors declare no competing financial interests. Correspondence and requests for materials should be addressed to W.R.B. (billboos@alum.mit.edu).

©2010 Macmillan Publishers Limited. All rights reserved

METHODS

Observational data. Boreal summer (June–August) climatologies for 1979–2002 of low-level wind and subcloud entropies were obtained from ERA40 (ref. 28), provided by NCAR. Subcloud entropies were obtained from four-times-daily values of temperature, specific humidity and pressure on model level 57 of the ERA40 data set, and these entropies were averaged in time and then converted to equivalent potential temperature (using definitions from ref. 30 of entropy and equivalent potential temperature). Four-times-daily horizontal winds at 850 hPa were averaged in time for this same period.

Twice-daily temperatures on the 200, 250, 300 and 400 hPa pressure levels from AIRS (level 3, version 5) were averaged in time (June–August, 2003–08) and in pressure to produce an upper-tropospheric mean temperature.

Estimates of precipitation for June–August, 1998–2006, were obtained from the TRMM 3B43V6 data set, also provided by NCAR. This data set consists of a monthly average of a precipitation product based on combined microwave and infrared satellite observations, adjusted over land to reduce the bias relative to rain gauges[32].

Radiosonde data were taken from the Integrated Global Radiosonde Archive[29], provided by the National Climatic Data Center. Only stations having data at both 00:00 and 12:00 UTC for June–August 1970–2008 were used, which limited the Tibetan plateau sites to those on the eastern half of the plateau. Temperatures and humidities were interpolated onto a 25 hPa vertical grid, and subcloud entropies were calculated using data from the lowest level of that grid above the station's surface level. CAPE and adiabatic temperature profiles were calculated according to the methodology given in ref. 30 using code provided by that author's website (http://wind.mit.edu/~emanuel).

Although different averaging periods were used for each of the above data sets based on their temporal coverage, our results proved insensitive to several changes in these averaging periods.

Model configuration. We used the CAM version 3.5.18 (ref. 31). This atmospheric GCM is an interim version of the model that has not been publicly released; it was chosen because the most recent public release (CAM 3.1) exhibited considerable bias in its simulation of the South Asian summer monsoon. In particular, subcloud entropies and upper-tropospheric temperatures in CAM 3.1 peaked over northwestern India and the Arabian peninsula in that model, about 1,000 km west of their positions in ERA40 data. One of the major differences between CAM 3.1 and CAM 3.5 is that the latter uses a finite volume instead of a spectral dynamical core. CAM 3.5 also represents vertical transports of horizontal momentum by cumulus convection, and enforces more entrainment of environmental air into cumulus updrafts in its convective parameterization.

The model was integrated at a horizontal resolution of 1.9×2.5 degrees with 26 vertical levels. All runs were started from initial conditions on 1 September 1992, and climatologies were taken for June–August over the following five summers. Results were typically clear after only one to two years of model time, which is why five years was deemed adequate as an integration period. The atmospheric GCM was coupled to an ocean surface with prescribed monthly SST and sea ice taken from the Smith/Reynolds analysed data set for the years 1992–97. We used five years of analysed SST instead of a cyclic SST climatology in order to provide some variability in the boundary conditions; the five years in each run might be viewed as five ensemble members. Over land, the model was coupled to the Community Land Model (CLM) version 3.5, which has ten soil layers and a zero heat flux boundary condition at the bottom of the soil column. Using a no-flux condition is important when performing runs with modified surface elevations, otherwise surface temperature would be partly controlled by the specification of temperature or heat flux at the bottom of the soil column.

Topography was modified by changing only the prescribed surface elevations. All other fixed properties of the surface, including soil colour and vegetation, were left unchanged. One integration was conducted with standard topography, another with all surface elevations set to zero, and a third with the surface elevation of the Tibetan plateau set to zero. In this last integration, topography between 75° E and 100° E was specified by setting surface elevations at each longitude to zero north of the point at which elevations reached two-thirds of their maximum at that particular longitude. Surface elevations in the ranges of (50°–60° E, 42°–90° N), (60°–75° E, 36°–90°N), and (100°–180° E, 29°–90° N) were also set to zero. These changes had the effect of removing the bulk of the Tibetan plateau while preserving a zonally elongated band of mountains to the south, east and west of the plateau. In all cases, whenever the surface elevation was reduced to zero, the prescribed subgrid scale elevation variance was also set to zero.

A model integration was also performed using standard topography but with the surface shortwave albedo set to unity for the Tibetan plateau, defined as the surface in Asia having pressures less than 600 hPa.

32. Huffman, G. *et al.* The TRMM Multisatellite Precipitation Analysis (TMPA): quasi-global, multiyear, combined-sensor precipitation estimates at fine scales. *J. Hydrometeorol.* **8**, 38–55 (2007).

©2010 Macmillan Publishers Limited. All rights reserved